

The Effects of High Magnetic Field Annealing on the Structural Relaxation of $\text{Fe}_{71}(\text{Nb}_{0.8}\text{Zr}_{0.2})_6\text{B}_{23}$ Bulk Metallic Glass

Peng Jia^a, En-gang Wang^{a*}

^aKey Laboratory of Electromagnetic Processing of Materials, Ministry of Education, Northeastern University, Shenyang 110819, China

Received: September 8, 2014; Revised: October 9, 2015

Fe-based magnetic metallic amorphous and nanocomposites have excellent soft magnetic properties including greater magnetization and magnetic permeability compared with crystalline alloys, especially at high operation frequency and temperature. The high magnetic field (HMF) up to 12T is introduced to the heat annealing of $\text{Fe}_{71}(\text{Nb}_{0.8}\text{Zr}_{0.2})_6\text{B}_{23}$ bulk metallic glass (BMG). The 12T HMF annealing shows the effect of improve the thermal stability of amorphous state during annealing in the BMG's supercooled liquid region as compared with the annealing without magnetic field. The HMF annealing inhibits the brittleness of BMG during the structural relaxation, due to the increment of the activation energy under the HMF. The HMF annealing also results in squared hysteresis loops after the structural relaxation and lower coercivity.

Keywords: *metallic glasses, soft magnetic property, high magnetic field, structural relaxation*

1. Introduction

In the past decades, Fe-based bulk metallic glasses (BMGs) with a high glass forming ability (GFA) have become a very hot research topic not only because of their soft-magnetic properties but also the high fracture strength and corrosion resistance¹⁻⁵. In particular, these BMGs can be obtained directly either from the liquid or the deformation within the supercooled liquid region in the final shape suitable for various applications in different devices, such as magnetic sensors, magnetic valves, and magnetic clutches etc. Soft magnetic materials with low core losses, high magnetization, and low cost are the key components for transformer with improved energy efficiency, especially in the higher frequency operation and elevated temperature conditions^{6,7}. Since the 1970s, the greatly reduced coercivity has been achieved in amorphous and nanocrystalline alloys⁸⁻¹². Conventional methods of improving the intrinsic and extrinsic soft magnetic properties have focused on tailoring the composition, controlling the microstructure with varied heat treatment environments. The low temperature annealing of metallic glass causes changes in most physics properties. This is attributed to atomic rearrangement in the amorphous state. Very recently, high magnetic field (HMF) up to above 10T has been successfully applied to materials design and productions^{13,14}. The finding has demonstrated that the magnetic field is a powerful tool to affect the crystallization process of metallic glass and texture formation of the crystallized phases¹⁵⁻²⁰. In this work, a HMF up to 12T is introduced to the low temperature structural relaxation process of high-boron $\text{Fe}_{71}(\text{Nb}_{0.8}\text{Zr}_{0.2})_6\text{B}_{23}$ BMG. The results show that HMF can improve the thermal stability of amorphous state during annealing in the BMG's supercooled liquid region as compared with the annealing without magnetic

field. The HMF annealing inhibits the brittleness of BMG during the structural relaxation, due to the increment of the activation energy under the HMF. The HMF annealing also results in lower coercivity and squared hysteresis loops of the metallic glass after structural relaxation.

2. Experimental

Elemental pieces with a purity better than 99.9 wt.% were used as starting materials. The master alloy ingots of $\text{Fe}_{71}(\text{Nb}_{0.8}\text{Zr}_{0.2})_6\text{B}_{23}$ with the nominal composition (in at.%) were prepared by arc melting under a Ti-gettered argon atmosphere. Bulk rods of 1.0 mm in diameter were fabricated using suction casting in a copper mold. The amorphous nature as well as homogeneity of the rod was ascertained with X-ray diffraction. The differential scanning calorimeter (DSC) measurements were performed under a purified Ar atmosphere in a TA Q100 at a heating rate of 2, 5, 10, 20 and 40 °C/min for both the as-cast and annealed samples. The morphology of the annealed rod was observed by using a scanning electron microscope (SEM). The magnetic field annealing was performed in a vacuum furnace, where a superconducting magnet (JMTD-12T100, JASTEC, Japan) was used to generate a magnetic field with a maximum magnetic flux density up to 12T at the center of a bore (100 mm in diameter). The 20-mm-length isothermal region of the furnace has an accuracy of around ± 3 °C. The stable homogeneous magnetic fields were used in this work. The axis of the rod was parallel to the direction of the magnetic field. As the magnetic field was applied, the samples were heated to a given temperature at a heating rate of 5 °C/min, kept for 60 minutes, and then cooled down to the temperature below 100 °C in the furnace. The average cooling rate is

*e-mail: egwang@mail.neu.edu.cn

around 6 °C/min. Vickers microhardness was measured in a MVR-HS hardness tester (Kawasaki, Japan) using a load of 300 N and 20 s hold time. The microhardness value given is the average of 20 individual measurements. Vibrating sample magnetometer (VSM, Lakeshore 7407) was used to measure the magnetic properties of the samples.

3. Results and Discussions

Figure 1 shows the DSC curves of the as-cast and annealed rods for $\text{Fe}_{71}(\text{Nb}_{0.8}\text{Zr}_{0.2})_6\text{B}_{23}$ BMG. Characteristic temperatures associated with the glass transition temperature (T_g) and the onset temperature of primary crystallization (T_{x1}) are labeled in Figure 1. To simulate the heating rate for the magnetic field annealing, a heating rate of 5 °C/min was used for the as-cast rod in the work¹⁵. At the heating rate of 5 °C/min, the T_g and T_{x1} of the as-cast rod are revealed to be 555 °C and 600 °C, respectively. Therefore, the structural relaxation annealing temperatures of this BMG are selected to be 500 °C and 550 °C, respectively.

The DSC curves of the samples both annealed at 500 °C for 60 min with or without a 12 T magnetic field are shown in Figure 1, which exhibit the significant endothermic characteristics of a glass transition followed by an exothermic peak almost with the same exothermic heat amount of the as-cast rod indicating the normally full amorphous structure after the low temperature annealing. From the XRD curves, no peak correspond to the crystalline phase is visible, which are not shown here. In contrast, there is no obvious T_g observed in the DSC curve of the sample annealed at 550 °C without the magnetic field and a following smaller exothermic heat amount which indicates a partial crystallization already occurred in the precursor sample. The endothermic enthalpy of sample annealed at 550 °C with 12T high magnetic field is higher than that without magnetic field, which showed that the HMF improved the thermal stability of amorphous state of $\text{Fe}_{71}(\text{Nb}_{0.8}\text{Zr}_{0.2})_6\text{B}_{23}$ BMG during the structural relaxation. Due to the partial crystallization when annealed at 550 °C, the structural relaxation discussed in this work focused on the rod annealed at 500 °C only.

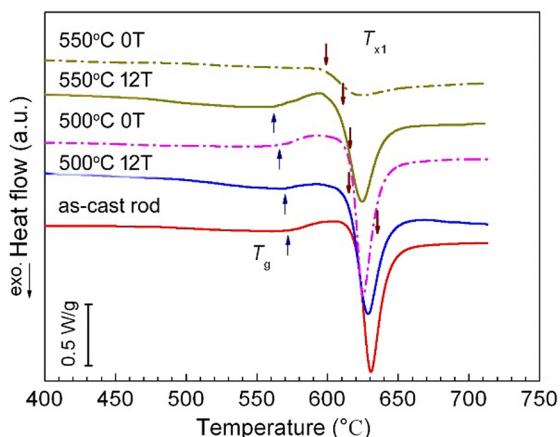


Figure 1. DSC traces for the $\text{Fe}_{71}(\text{Nb}_{0.8}\text{Zr}_{0.2})_6\text{B}_{23}$ BMG after annealing for 1h at different states at the heating rate of 20 °C/min.

The continuous DSC traces of the as-cast and annealed rods at 500 °C with heating rate of 2, 5, 10, 20 and 40 °C/min are done which are not shown here. The T_g , T_{x1} , and T_p (peak temperature of primary crystallization) of the rods are shifted to a higher temperature by increasing heating rate. The Kissinger plots of the primary and peak crystallization reactions for the three rods are shown in Figure 2. The activation energy E_x and E_p are deduced from the slope of $-\ln(R/T^2)$ versus $1/T$, where T stands for the T_{x1} , and T_p , R stands for the heating rate. The E_x and E_p for the as-cast rod are 508.2 and 528.5 kJ/mol, respectively. The E_x and E_p are enhanced after annealed at 500 °C without magnetic field, which are 520.0 and 531.4 kJ/mol, respectively. However, the E_x and E_p increased dramatically after annealed at 500 °C with 12T high magnetic field, which are 586.8 and 541.4 kJ/mol, respectively, and the E_p is lower than E_x , which is different from of as-cast rod and annealed without magnetic field. From the DSC curves in Figure 1, the improved thermal stability of $\text{Fe}_{71}(\text{Nb}_{0.8}\text{Zr}_{0.2})_6\text{B}_{23}$ BMG during HMF annealing assumed ascribing to the increased E_x .

The indentation of the BMG rods after structural relaxation is also investigated. In comparison, the indentation results of BMG rods annealed at higher temperature are also presented in Figure 3a. It is clearly seen that the hardness is higher in the rod annealed without magnetic field compared that with 12T HMF. For the rods (A and B as shown in Figure 3a after structural relaxation, the indentation images are also show in Figure 3b and 3c, respectively. Shear bands around the indentation are clearly seen in the rod annealed with 12T, which showing the higher plasticity, in contrast with that annealed without magnetic field.

The effect of the field annealing on the hysteresis loops of the $\text{Fe}_{71}(\text{Nb}_{0.8}\text{Zr}_{0.2})_6\text{B}_{23}$ BMG is demonstrated in Figure 4. It is evident that the HMF annealing increase the saturation magnetization compared with those of annealing without magnetic field and as-cast rods. The different magnetization process indicates that the domains rotate easily by external field due to low anisotropy. While, saturation field is lowest in the rod annealed under 12 T, indicating the lowest anisotropy. Therefore, the coercivity field is also deduced from 30.5 A/m in the rod annealed without external field to 10.6 A/m in the rod annealed under 12 T.

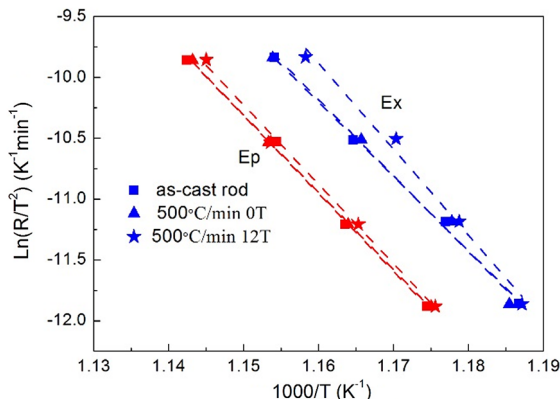


Figure 2. Kissinger plots of the start and peak temperatures for the primary crystallization for $\text{Fe}_{71}(\text{Nb}_{0.8}\text{Zr}_{0.2})_6\text{B}_{23}$ BMG.

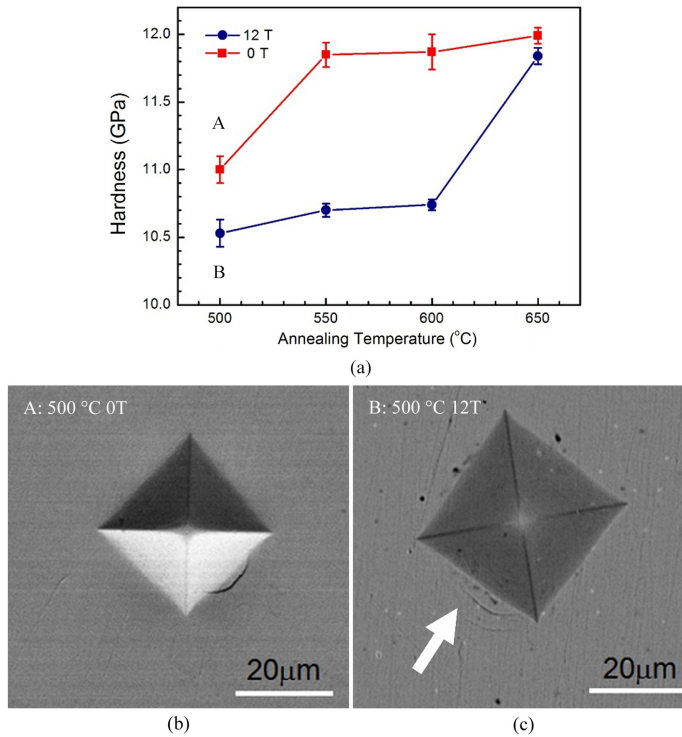


Figure 3. (a) Hardness as a function of annealing temperature in $\text{Fe}_{71}(\text{Nb}_{0.8}\text{Zr}_{0.2})_6\text{B}_{23}$ BMG annealed under 0 T and 12 T magnetic field. The corresponding indentation images for the rod annealed at (b) 500 °C under 0T and (c) 500 °C under 12T external field.

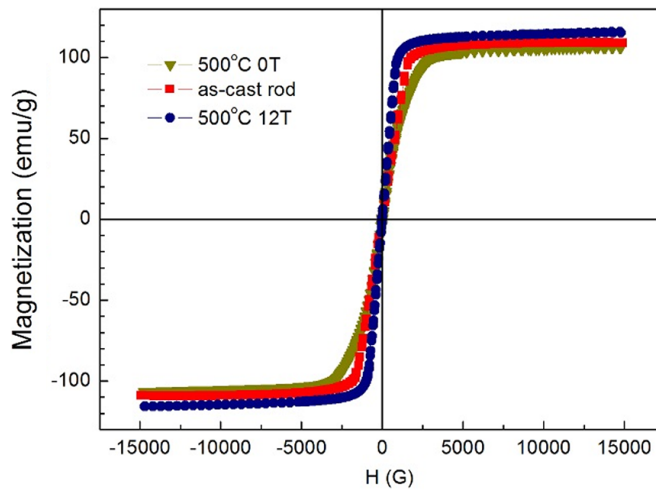


Figure 4. Hysteresis loops for $\text{Fe}_{71}(\text{Nb}_{0.8}\text{Zr}_{0.2})_6\text{B}_{23}$ BMG after annealing for 1h at different states.

4. Conclusions

- (1) HMF can improve the thermal stability of amorphous state during structural relaxation annealing in the BMG's supercooled liquid region as compared with the annealing without magnetic field for $\text{Fe}_{71}(\text{Nb}_{0.8}\text{Zr}_{0.2})_6\text{B}_{23}$ bulk metallic glass.
- (2) HMF can effectively suppress the brittleness of $\text{Fe}_{71}(\text{Nb}_{0.8}\text{Zr}_{0.2})_6\text{B}_{23}$ bulk metallic glass during structural relaxation.

- (3) HMF can reduce the coercivity and saturation magnetization, which is thought due to the reduced anisotropy by high magnetic field annealing.

Acknowledgements

This work was supported by the National Natural Science Foundation of China (Grant Nos. 51104047 and 51171041) and the 111 Project of China (No. B07015).

References

- Inoue A, Shen BL and Chang CT. Super-high strength of over 4000 MPa for Fe-based bulk glassy alloys in [(Fe_{1-x}Co_x)_{0.75}B_{0.2}Si_{0.05}]_{0.96}Nb₄ system. *Acta Materialia*. 2004; 52(14):4093-4099. <http://dx.doi.org/10.1016/j.actamat.2004.05.022>.
- Gu XJ, Poon SJ, Shiflet GJ and Widom M. Ductility improvement of amorphous steels: roles of shear modulus and electronic structure. *Acta Materialia*. 2008; 56(1):88-94. <http://dx.doi.org/10.1016/j.actamat.2007.09.011>.
- Yao JH, Wang JQ and Li Y. Ductile Fe-Nb-B bulk metallic glass with ultrahigh strength. *Applied Physics Letters*. 2008; 92(25): 251906.
- Li HX, Jiao ZB, Gao JE and Lu ZP. Synthesis of bulk glassy Fe-C-Si-B-P-Ga alloys with high glass-forming ability and good soft-magnetic properties. *Intermetallics*. 2010; 18(10):1821-1825. <http://dx.doi.org/10.1016/j.intermet.2010.01.021>.
- Wang JF, Li R, Hua NB, Huang L and Zhang T. Ternary Fe-P-C bulk metallic glass with good soft-magnetic and mechanical properties. *Scripta Materialia*. 2011; 65(6):536-539. <http://dx.doi.org/10.1016/j.scriptamat.2011.06.020>.
- Gutfleisch O, Willard MA, Brück E, Chen CH, Sankar SG and Liu JP. Magnetic materials and devices for the 21st century: stronger, lighter, and more energy efficient. *Advanced Materials*. 2011; 23(7):821-842. <http://dx.doi.org/10.1002/adma.201002180>. PMID:21294168.
- Willard MA, Daniil M and Knipping KE. Nanocrystalline soft magnetic materials at high temperatures: a perspective. *Scripta Materialia*. 2012; 67(6):554-559. <http://dx.doi.org/10.1016/j.scriptamat.2011.12.043>.
- Shen BL, Akiba M and Inoue A. Excellent soft-ferromagnetic bulk glassy alloys with high saturation magnetization. *Applied Physics Letters*. 2006; 88(13):131907. <http://dx.doi.org/10.1063/1.2189910>.
- Chang CT, Shen BL and Inoue A. FeNi-based bulk glassy alloys with superhigh mechanical strength and excellent soft-magnetic properties. *Applied Physics Letters*. 2006; 89(5):051912. <http://dx.doi.org/10.1063/1.2266702>.
- Suzuki K, Makino A, Inoue A and Masumoto T. Low core losses of nanocrystalline Fe-M-B (M=Zr, Hf, or Nb) alloys. *Journal of Applied Physics*. 1993; 74(5):3316-3322. <http://dx.doi.org/10.1063/1.354555>.
- McHenry ME, Johnson F, Okumura H, Ohkubo T, Ramanan VRV and Laughlin DE. The kinetics of nanocrystallization and microstructural observations in FINEMET, NANOPERM and HITPERM nanocomposite magnetic materials. *Scripta Materialia*. 2003; 48(7):881-887. [http://dx.doi.org/10.1016/S1359-6462\(02\)00597-3](http://dx.doi.org/10.1016/S1359-6462(02)00597-3).
- McHenry ME, Willard MA and Laughlin DE. Amorphous and nanocrystalline materials for applications as soft magnets. *Progress in Materials Science*. 1999; 44(4):291-433. [http://dx.doi.org/10.1016/S0079-6425\(99\)00002-X](http://dx.doi.org/10.1016/S0079-6425(99)00002-X).
- Zhou ZN and Wu KM. Molybdenum carbide precipitation in an Fe-C-Mo alloy under a high magnetic field. *Scripta Materialia*. 2009; 61(7):670-673. <http://dx.doi.org/10.1016/j.scriptamat.2009.05.021>.
- Li X, Ren ZM, Fautrelle Y, Zhang YD and Esling C. Morphological instabilities and alignment of lamellar eutectics during directional solidification under a strong magnetic field. *Acta Materialia*. 2010; 58(4):1403-1417. <http://dx.doi.org/10.1016/j.actamat.2009.10.048>.
- Jia P, Liu JM, Wang EG and Han K. The effects of high magnetic field on crystallization of Fe₇₁(Nb_{0.8}Zr_{0.2})₆B₂₃ bulk metallic glass. *Journal of Alloys and Compounds*. 2013; 581:373-377. <http://dx.doi.org/10.1016/j.jallcom.2013.07.066>.
- Suzuki K, Ito N, Garitaonandia JS and Cashion JD. High saturation magnetization and soft magnetic properties of nanocrystalline (Fe,Co)₉₀Zr₈B₃ alloys annealed under a rotating magnetic field. *Journal of Applied Physics*. 2006; 99(8):08F114:1-3. <http://dx.doi.org/10.1063/1.2169503>.
- Fujii H, Tsurekawa S, Matsuzaki T and Watanabe T. Evolution of a sharp 110 texture in microcrystalline Fe₇₈Si₉B₁₃ during magnetic crystallization from the amorphous phase. *Philosophical Magazine Letters*. 2006; 86(2):113-122. <http://dx.doi.org/10.1080/09500830600582858>.
- Zhuang YX, Chen J, Liu WJ and He JC. Effect of high magnetic field on crystallization of Zr_{46.75}Ti_{8.25}Cu_{7.5}Ni₁₀Be_{27.5} bulk metallic glass. *Journal of Alloys and Compounds*. 2010; 504:s256-s259. <http://dx.doi.org/10.1016/j.jallcom.2010.02.166>.
- Wang XD, Qi M and Yi S. Crystallization behavior of bulk amorphous alloy Zr₆₂Al₈Ni₁₃Cu₁₇ under high magnetic field. *Scripta Materialia*. 2004; 51(11):1047-1050. <http://dx.doi.org/10.1016/j.scriptamat.2004.08.011>.
- Yoshizawa Y, Fujii S, Ping DH, Ohnuma M and Hono K. Magnetic properties of nanocrystalline FeMCuNbSiB alloys (M: Co, Ni). *Scripta Materialia*. 2003; 48(7):863-868. [http://dx.doi.org/10.1016/S1359-6462\(02\)00611-5](http://dx.doi.org/10.1016/S1359-6462(02)00611-5).